SEMARAK ILMU PUBLISHING

CFD Letters

Journal homepage:
https://semarakilmu.com.my/journals/index.php/CFD_Letters/index
ISSN: 2180-1363

Velocity and Thermal Slips Impact on the Williamson Fluid Flow above a Stretching Sheet in the Existence of Radiation and Inclined Magnetic Field

Anagandula Srinu[1,*], K. Sreeram Reddy[1]

[1] Department of Mathematics, University College of Science, Osmania University, Hyderabad-500007, Telangana, India

ARTICLE INFO

Article history:
Received 8 September 2023
Received in revised form 10 October 2023
Accepted 12 November 2023
Available online 29 February 2024

Keywords:
Williamson fluid; bvp4; Radiation; inclined magnetic field; Thermal Slips

ABSTRACT

Research has been conducted on the study of the velocity and thermal slips' impact on the Williamson fluid flow above a stretching sheet in the existence of an inclined magnetic field and Radiation. By applying the proper similarity conversions, the governing equations (PDEs) are reduced to a set of non-linear ODEs, and a numerical solution is produced by using MATLAB in-built solver bvp4c package. The impacts of the dimensionless characteristics on the flow patterns are analyzed visually, and the values of the friction, Nusselt, and mass transfer quantities are tabulated to exemplify how the various physical factors have an influence. We noted that the velocity profile enhances the rising estimations of velocity slip and the temperature profile increases with Q increase.

1. Introduction

Non-Newtonian fluids are distinguished from Newtonian fluids by their nonlinear connection between stress and strain. Newtonian fluids are the most fundamental form of fluid. This category of fluids is something that we could come across in the path of our everyday lives. For instance, toothpaste, crude oil, honey, paint, and a variety of other things. The study of such fluids is necessary in the modern world because of how quickly things are evolving. Numerous academics have been putting in a lot of work to try to forecast the proper mathematical models for the various non-Newtonian fluids that exist. To this point, a variety of models for non-Newtonian fluids have been presented, and those models' flow properties, including flow, heat transfer, and mass transfer across stretched surfaces, have been explored. According to the research published by Choi [1], nanoparticles improve the thermal efficiency of nanofluids in comparison to the base fluid. The temperature dependency of the heat transfer increase in nanofluids was investigated by Das *et al.,* [2]. Khan and Pop [3] have demonstrated the boundary-layer flow of a nanofluid in the vicinity of a stretching sheet. The Critical evaluation of heat transfer properties of nanofluids was analyzed by Trisaksri and Wongwises [4]. Bachok *et al.,* [5] demonstrated the constant boundary-layer movement of a nanofluid in a constant free stream as it moved past a moving semi-infinite flat plate. A

* *Corresponding author.*
E-mail address: daruvusrinu@gmail.com (Anagandula Srinu)

https://doi.org/10.37934/cfdl.16.7.118135

computational analysis was conducted by Rana and Bhargava [6] to investigate the flow and heat transport of a nanofluid across a nonlinearly stretched sheet. Hassani [7] investigated a nanofluid boundary layer flow across a stretched sheet analytically. The impacts of slip and convection circumstances on the MHD flow of nanofluid across a permeable nonlinear stretched surface were examined by Daniel *et al.,* [8].

When there is a difference in temperature between the heat of the flow separation sheet and the fluid properties in the surrounding region, the impact of thermal radiation is quite significant and has a significant influence. The radioactive rates of heat exchange effects have significant repercussions for both the field of engineering technology and the field of physics. These technologies include things like hypersonic aircraft, nuclear power plants, launch systems, and extreme temperature systems, to name a few examples. Thermal radiation plays an important role in the transmission of electricity in a variety of applications, including combustion furnaces, fires, nuclear explosions, and chambers. This is because thermal radiation is a kind of electromagnetic radiation. Nanofluid flow across a stretched surface with heat radiation was studied by Kalidas Das *et al.,* [9]. Boundary layer flow and heat transport of a nanofluid across a permeability unstable stretched surface with viscous dissipation were studied by Ferdows *et al.,* [10]. The influences of radiation on the heat transmission and the flow of an MHD nanofluid over parallel plates were investigated by Dogonchi *et al.,* [11]. A thermal and mass transmission examination was performed on the MHD flow of nanofluid while radiation absorption was taken into consideration was investigated by Durga Prasad *et al.,* [12].

Almost all fluids that are not Newtonian fall into one of three categories: continuous, rate, or divergence. The Maxwell fluid is a nonviscous rate-type fluid. These young people exemplify the effects of free time. There are two types of non-Newtonian fluids: those that are time-dependent and those that are not. Williamson fluid is a non-Newtonian fluid with pseudo-plastic properties that do not depend on the passage of time. Multiple applications in manufacturing and engineering rely on non-Newtonian nanofluid boundary flow across a linear surface, such as image generation and data extraction from polymer surfaces. In their study, Williamson nanofluids were studied by Ibrahima and Gamachu [13], who looked at their nonlinear convection flow as it moved over a radially extending surface. Nadeem *et al.,* [14] looked at the flow of a Williamson fluid through a stretched sheet as part of their research. Srinivasulu and Goud [15] studied the impact that an inclined magnetic field had on the flow, flow of heat, and transport phenomena of a Williamson nanofluid through a stretching sheet. Williamson fluid thin film flows across a non-uniformly stretched permeable sheet was investigated by Zahir Shah *et al.,* [16]. Malik and Salahuddin [17] investigated approximate solutions for the MHD stagnation point flow of the Williamson flow characteristics across a stretched cylinder. In the presence of heat radiation and Ohmic, the hydromagnetic boundary layer flow of Williamson fluid was addressed by Hayat *et al.,* [18]. The statistical research of Williamson fluid boundary layer flow concerning a radiative surface was conducted by AnumShafiq and Sindhu [19]. Investigation of the influence of radiation on MHD flow and heat transfer in a Williamson nanofluid using a stretched sheet maintained at a constant temperature was studied by Kho *et al.,* [20]. The Williamson fluid stream caused by a nonlinearly extending sheet, including radiation and dissipation was investigated by Megahed [21]. Many authors studied the porous surface Rana *et al.,* [25], Dadheech *et al.,* [26] examined the Williamson fluid over a vertical plate, Salahuddin *et al.,* [27] investigated the Carreau fluid over a radiated cylinder, Goud BS [28] examined Soret and Dufour effects on a permeable plate, Srisailam *et al.,* [29] studied on MHD fluid flow, Jaffrullah et [30] examined the Joule heating influence on Forchheimer permeable medium, Kota[31] studied with viscous dissipation and heat source embedded in a porous medium, Bejawada *et al.,* [32] examined the free convection on a vertical stretching surface with suction and blowing, Iyoko *et*

al., [33]studied the Jeffery Fluid over Stretching Sheet, GoudB [34] investigated the solution of thermostatically stratified fluid with dissipation impact, and Usman [35] examined the Casson fluid flow past a permeable.

The work of the aforementioned scientists and engineers has inspired this discussion and investigation of the impact of slips and thermal radiation on Williamson fluid flow above a stretched sheet in the existence of an inclined magnetic field. The governing PDEs are first translated into ODEs, before being solved numerically by employing the bvp4c approach for certain values of the governing parameters. As far as the authors are aware, no other published research has ideas that are similar to those in this paper. The novelty of this study is based on the efficiency of heat generation caused by nanoparticle movements in the presence of slip conditions.

2. Formulation

The MHD inviscid flow, thermal, and concentration boundary layers are all shown in Figure 1. Using boundary layer theory, a surface that is stretching with a particular velocity $U_w(x) = ax$, and temperature $T_w$may be characterized and pretend that the temperature of the ambient fluid, T_∞ are modeled as Williamson nanofluids on the surface, respectively. The flow is controlled such that $y > 0$. The magnetic field is applied to the fluid flow in a direction that is orthogonal to the x −axis after an angle "α" is taken with it. The induced magnetic field is not taken into account and is predicted to be much less in comparison to the applied magnetic field that is also not taken into account, and the flow model for the problem can be viewed in Figure 1.

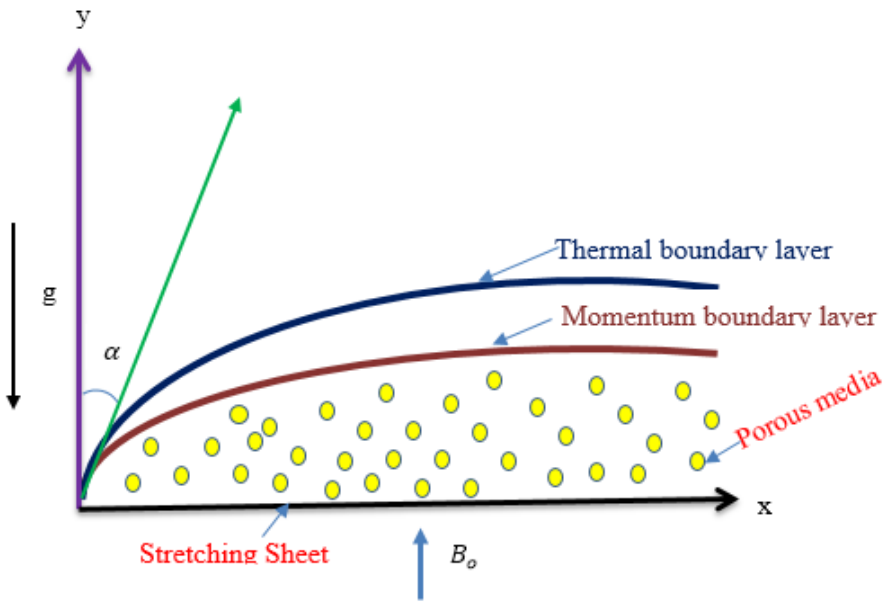

Fig. 1. Flow geometry

The Williamson fluid model that Nadeem and Hussain [15] used is taken into consideration. The Cauchy stress tensor, denoted by S, is defined as follows in the context of the current fluid model:

$$s = -pI + \tau_1$$
$$S = -pI = \left(\mu_\infty + \frac{\mu_o - \mu_\infty}{1 - \Gamma\alpha}\right) A_1$$

Where $\Gamma > 0$ is referred to as constant time &γ can be specified as $\alpha = \sqrt{\frac{\pi}{2}}$, $\pi = trace(A_1^2)$,

$$\alpha = \sqrt{\left(\frac{\partial u}{\partial x}\right)^2 + \frac{1}{2} + \left(\frac{\partial u}{\partial y} + \frac{\partial v}{\partial x}\right)^2 + \left(\frac{\partial v}{\partial y}\right)^2}$$

In this particular instance, we focused on the $\mu_\infty = 0, \Gamma\alpha < 1$ situation.

Then, we achieved $\tau_1 = \left(\frac{\mu_0 A_1}{1-\Gamma\alpha}\right)$ or $\tau_1 = \left(\mu_0 A_1 (1 - \Gamma\alpha)\right)$

Following these presumptions, we get the following set of governing equations [15]:

$$\frac{\partial u}{\partial x} + \frac{\partial v}{\partial y} = 0 \tag{1}$$

$$u\frac{\partial u}{\partial x} + v\frac{\partial u}{\partial y} = \upsilon\frac{\partial^2 v}{\partial y^2} + \sqrt{2}\upsilon\Gamma\frac{\partial u}{\partial y}\frac{\partial^2 u}{\partial y^2} - \frac{\sigma B_0^2}{\rho_f}\sin^2(\alpha)\, u + \frac{\nu}{K^*}u \tag{2}$$

$$u\frac{\partial T}{\partial x} + v\frac{\partial T}{\partial y} = \frac{k}{(\rho C_p)_f}\frac{\partial^2 T}{\partial y^2} + \frac{1}{(\rho C_p)_f}\frac{16\sigma^* T_\infty^3}{3K^*}\frac{\partial^2 T}{\partial y^2} + \frac{\sigma B_0^2}{(\rho C_p)_f}u^2 + \frac{\upsilon}{C_p}\left[\left(\frac{\partial u}{\partial y}\right)^2 + \sqrt{2}\Gamma\left(\frac{\partial u}{\partial y}\right)^3\right] + Q_o(T - T_\infty) \tag{3}$$

$$\left.\begin{array}{l} u_w = u = ax + A^*\frac{\partial u}{\partial y}, v = v_w, T = T_w + B^*\frac{\partial T}{\partial y}, at\ y \to 0 \\ u = 0, \quad T = T_\infty, \qquad\qquad as\ \ y \to \infty \end{array}\right\} \tag{4}$$

Following is a conversion of the similarity variables:

$$\left.\psi = \sqrt{a\upsilon} f(\eta), \eta = y\sqrt{\frac{a}{\upsilon}}, \theta(\eta) = \frac{T - T_\infty}{T_f - T_\infty}\right\} \tag{5}$$

The formula for the stream function ψ as $u = \frac{\partial \psi}{\partial y}$, &$v = -\frac{\partial \psi}{\partial x}$ also, nondimensional stream, thermal, and concentration functions can be defined as $f(\eta)$, $\theta(\eta)$ and $\phi(\eta)$ respectively.

The ODEs are obtained by substituting Eq. (5) into the governing Eq. (2)-(4):

$$(1 + \lambda f'')f''' + ff'' - (f')^2 - (\mathrm{M}\sin^2(\alpha) + K_p)f' = 0 \tag{6}$$

$$\theta'' + \frac{Pr}{(1+R)}[f\theta' + Ec((f'')^2 + We(f'')^3 + Mf'^2) + Q\theta] = 0 \tag{7}$$

From Eq. (4), the dimensionless BCs become

$$\left.\begin{array}{l} f = f_w, f'(\eta) = 1 + Af''(0),\ \theta(0) = 1 + \delta\theta'(0),\ at\ \eta \to 0 \\ f' \to 0,\ \theta \to 0, \qquad\qquad as \quad \eta \to \infty \end{array}\right\} \tag{8}$$

Here, the limitation conditions are specified as:

$$\left.\begin{array}{l} M=\frac{\sigma B_0^2}{\rho_f a}, Pr=\frac{k}{(\rho C_p)_f}, \lambda=\sqrt{\frac{2a}{\upsilon}}ax\Gamma, R=\frac{16\sigma^* T_\infty^3}{3kk^*}, f_w=-\frac{v_w}{\sqrt{a\upsilon}}, \\ We=x\Gamma\sqrt{\frac{2a^3}{\upsilon}}, Ec=\frac{u_w^2}{C_p(T_f-T_\infty)}, \ \ Le=\frac{\upsilon}{D_B}, A=A^*\sqrt{\frac{a}{\upsilon}}, \delta=B^*\sqrt{\frac{a}{\upsilon}} \end{array}\right\} \quad (9)$$

The skin friction, local Nusselt number, and local Sherwood number can be defined as:

$$C_{f_x}=\frac{\tau_w}{\rho u_w^2}, \& \ Nu_x=\frac{xq_w}{k(T-T_w)} \quad (10)$$

At the surface, the shear stress,

$$\tau_w=\mu\left[\frac{\partial u}{\partial y}+\frac{\Gamma}{\sqrt{2}}\left(\frac{\partial u}{\partial y}\right)^3\right], \text{ and thermal flux} q_w=-k\left(\frac{\partial T}{\partial y}\right)_{y=0} \quad (11)$$

Using Eq. (5) to solve for variables in Eq. (10) and Eq. (11), we get the following terms:

$C_{f_x}\sqrt{Re_x}=\left(1+\frac{\lambda}{2}f''(0)\right)f''(0)$, $\frac{Nu_x}{\sqrt{Re_x}}=-(1+R)\theta'(0)$, Here the local Reynolds number specified as $Re_x=\frac{u_w x}{\upsilon}$.

3. Numerical method

The transformed set of ODE Eq. (6)-(7) and the appropriate boundary circumstances Eq. (8) have been solved numerically by using the bvp4c technique the programming pattern of the boundary circumstances can be employed to determine three unknowns. The procedure will be performed before the desired extent of accuracy is obtained. Reduce the Eq. (8)-(9) in to set of first-order equations via proper substitution defined as follows:

$$\text{ﻑ}(1)=\text{ﻑ}(\eta), \text{ﻑ}(2)=\text{ﻑ}'(\eta), \text{ﻑ}(3)=\text{ﻑ}''(\eta), \text{ﻑ}(4)=\theta(\eta), \text{ﻑ}(5)=\theta'(\eta),$$

Now, the subsequent set of equations of the first order are as follows:

$$\begin{pmatrix} \text{ﻑ}'(1) \\ \text{ﻑ}'(2) \\ \text{ﻑ}'(3) \\ \text{ﻑ}'(4) \\ \text{ﻑ}'(5) \end{pmatrix}=\begin{pmatrix} \text{ﻑ}(2) \\ \text{ﻑ}(3) \\ -\frac{\left(\text{ﻑ}(1)*\text{ﻑ}(3)-\left(\text{ﻑ}(2)\right)^2+(\mathrm{Msin}^2(\alpha)+K_p)*\text{ﻑ}(2)\right)}{\left(1+\lambda\text{ﻑ}(3)\right)} \\ \text{ﻑ}(5) \\ \left(\frac{-\mathrm{Pr}}{1+R}\right)\left(\text{ﻑ}(1)*\text{ﻑ}(5))+Ec\left(\left(\text{ﻑ}(3)\right)^2+We\left(\text{ﻑ}(3)\right)^2+M\left(\text{ﻑ}(2)\right)^2+Q\text{ﻑ}(4)\right)\right) \end{pmatrix}$$

The associated initial conditions are:

$$\begin{pmatrix} \not{f}_a(1) \\ \not{f}_a(2) \\ \not{f}_a(4) \\ \not{f}_a(2) \\ \not{f}_a(6) \end{pmatrix} = \begin{pmatrix} f_w \\ -1 - A * \not{f}_a(3) \\ -1 - \delta * \not{f}_a(5) \\ 0 \\ 0 \end{pmatrix}$$

In this article, a step size of 0.01 is selected to satisfy the convergence criterion of 10^{-4} . In the results, six decimal places of accuracy are obtained**.**

4. Numerical code Validation

Comparison values of Skinfriction with Pr. Enhanced skin friction numerical results for various fluids and has shown the validity of the method. Parameters are summed up as Table 1 uses the numbers from Khan and Pop [22], Gorla &Sidawi [23], and Wang [24] to draw comparisons between the three studies. It demonstrates the precision expected. A verification code is thus allowed.

Table 1
Comparison of values of $-\theta'(0)$with previous results when $\lambda = R = Ec = M = Kp = \alpha = f_w = A = \delta = 0$

Pr	Khan and Pop [22]	Gorla and Sidawi [23]	Wang [24]	Present study
0.7	0.4539	0.4539	0.4539	0.4539
2	0.9113	0.9114	0.9114	0.9113
7	1.8954	1.8905	1.8954	1.8954

5. Graphical Results and Discussion

Figure 2 shows that the influence of a magnetic field factor on velocity gradient. A drag force is known as the Lorentz force and it is improved by governing the magnetic field because this boundary layer surface is attracted towards the velocity and hence the width lowers as magnetic strength is higher.

Figure 3 illustrates the impact that the parameter representing the magnetic field has on the temperature. As the magnetic field parameter M rises, there is a corresponding rise in temperature profile. In addition to this, we can observe that the thickness of the thermal boundary layer grows when the magnetic field value is raised.

Figure 4 shows the variations in the velocity field for several values of the suction/injection parameter (fw). The increase in wall suction causes an increase in velocity, causing the flow to accelerate. Suction increases the boundary layer's adherence to the flow, lowering the thickness of the momentum boundary layer. As a result, suction can also be used to stabilize the outside flow of the boundary layer on the wedge surface. However, increasing the injection factor at the wedge's wall causes to the flow decelerate significantly, i.e. the pressure drop. As assumed, the fluid velocity for impermeable wedges drops between the weak suction/injection instances.

Table 2

The quantities of $C_{f_x}\sqrt{Re_x}$, and $Nu_x(Re_x)^{-1/2}$ with various values of M, f_w, Kp, λ and α the other values are $Pr = 7, Ec = 0.2, We = 3, Q = 0.2, \lambda = 0.1, \delta = 0.1, R = 0.2$

M	f_w	Kp	A	α	$-\left(1+\frac{\lambda}{2}f''(0)\right)f''(0)$	$-(1+R)\theta'(0)$
1	0.1	0.1	0.1	$\pi/6$	0.481335	1.909836
2					0.515432	1.736706
3					0.545857	1.602261
1	0.3				0.516762	2.832506
	0.5				0.553765	3.692629
	0.1	0.3			0.508936	2.014749
		0.5			0.534073	2.118347
		0.1	0.3		0.386495	1.481884
			0.5		0.325461	1.268373
				$\pi/4$	0.515432	2.040768
				$\pi/3$	0.545857	2.169733

Table 3

The quantities of $Nu_x(Re_x)^{-1/2}$ with various values of Pr, Ec, We, Q, R, and δ and α the other values are $M = 1, f_w = 0.1, \alpha = \pi/6, Kp = 0.1$, and $\lambda = 0.1$

Pr	Ec	We	Q	R	δ	$-(1+R)\theta'(0)$
3	0.2	1	0.2	0.2	0.1	0.673414
5						0.982348
7						1.215433
3	0.4					0.441143
	0.6					0.208872
	0.2	3				1.017602
		5				1.361791
		1	0.3			0.426488
			0.4			0.005372
			0.2	0.3		0.681152
				0.4		0.686023
				0.2	0.3	0.585095
					0.5	0.517256

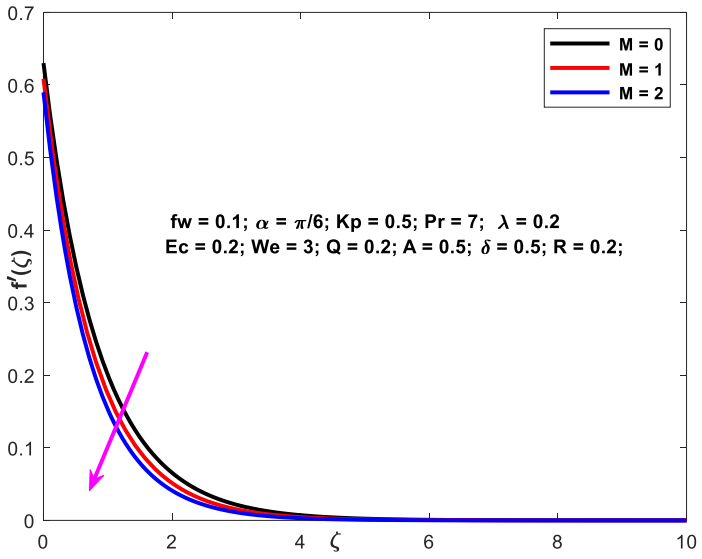

Fig. 2. $f'(\zeta)$ vs M

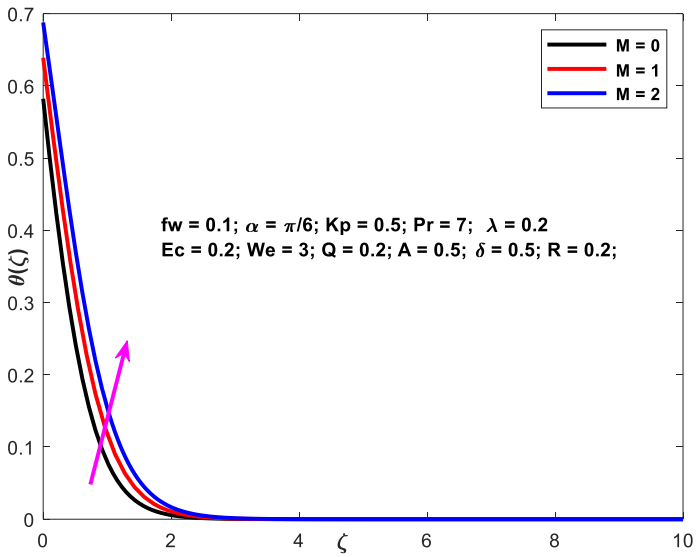

Fig. 3. $\theta(\zeta)$ vs M

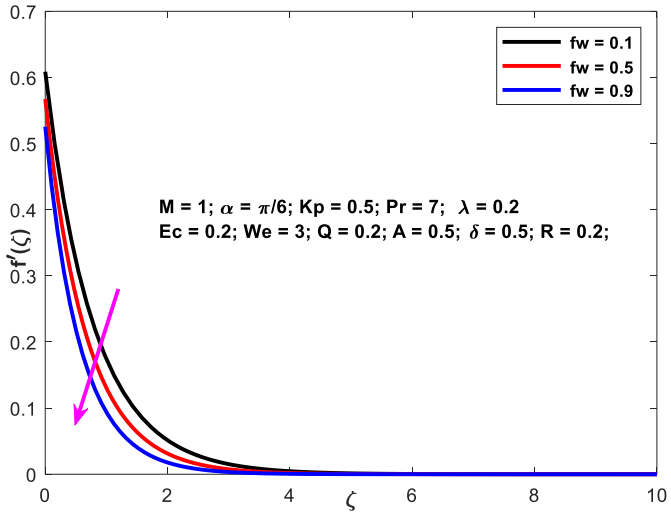

Fig. 4. $f'(\zeta)$ vs fw

Figure 5 demonstrates the variations in the thermal field with several values of the suction/injection constraint (fw). Temperature upsurges with injection and declines with suction. When suction is increased, the thickness of the temperature curves falls. Furthermore, increases in heat transformations from the wall to the field, result in a drop in temperature. As a result, we can conclude that the suction mechanism may be advantageous for rapidly cooling the flow field. Additionally, it is possible to perceive that a solid injection raises the thickness of the thermal boundary layer. It is primarily because the injection tries to force the heated fluid extracted from the wall, forming a separating layer with a temperature close to that of the wall.

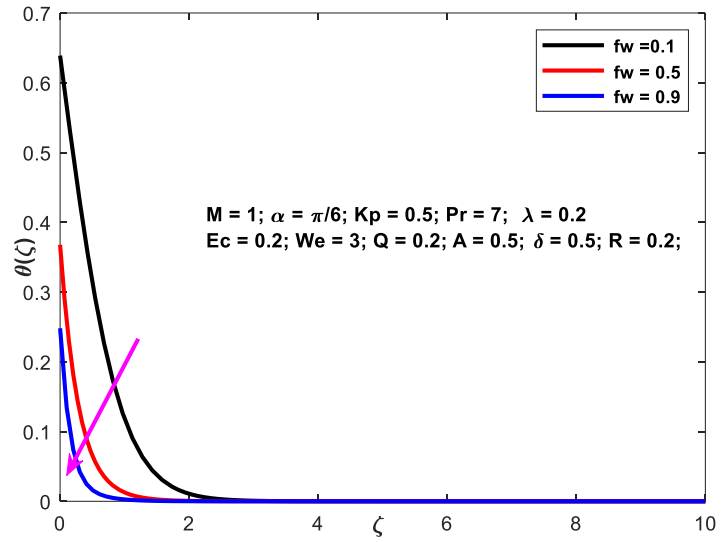

Fig. 5. $\theta(\zeta)$ vs fw

The variation of the profiles of velocity as well as temperature in contrast to the angle of inclination factor is shown in Figures 6 and Figure 7. If one looks at the graph, one can notice that a rise in the component results in a drop in velocity while an enhancement in temperature gradients.

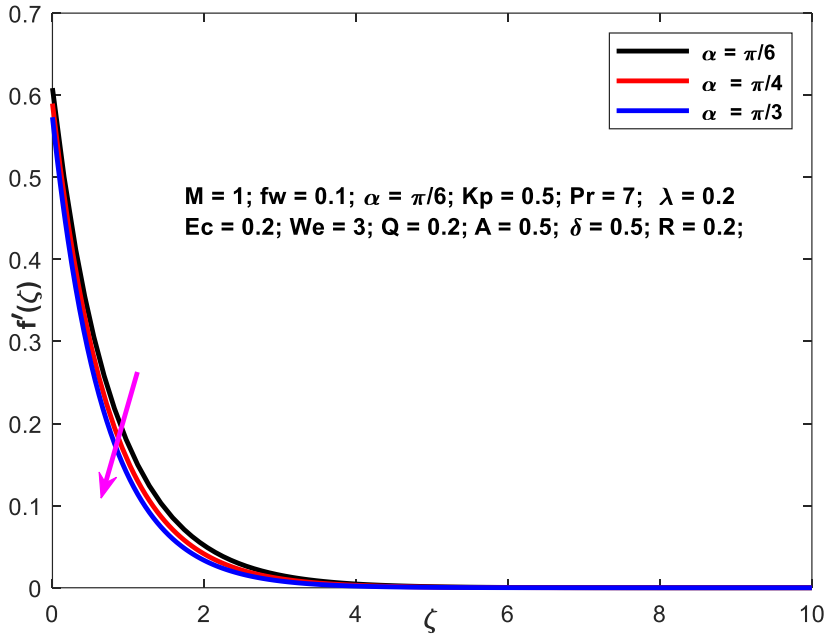

Fig. 6. $f'(\zeta)$ vs α

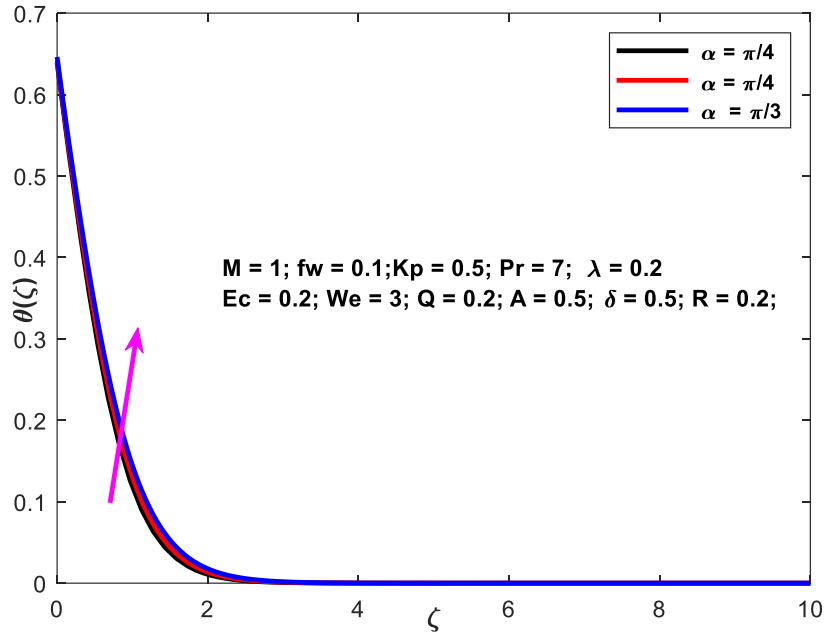

Fig. 7. $\theta(\zeta)$ vs α

Distributions of velocity and temperature vs permeability factor K are shown in Figure 8 and Fifure 9, respectively. Enhancing the permeability variable leads to a fall in velocity and an upsurge in temperature.

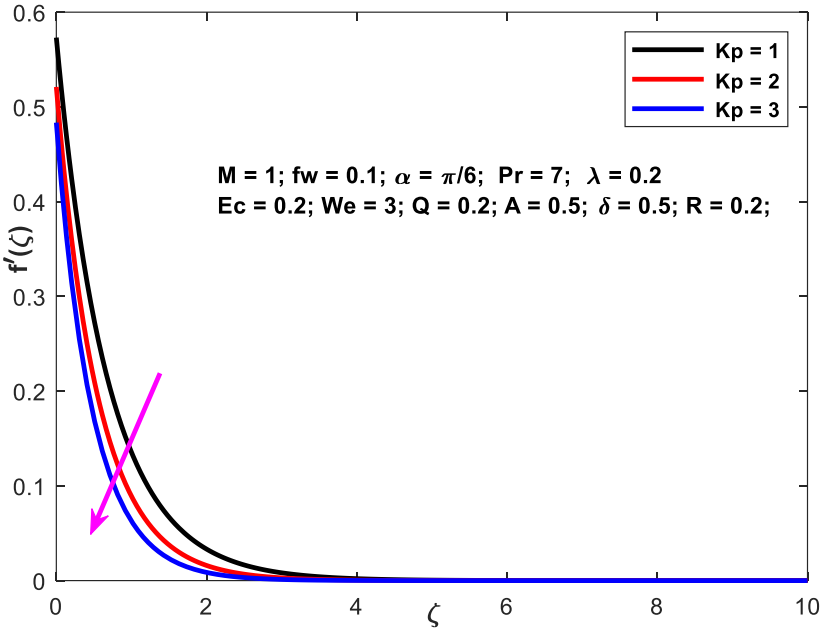

Fig. 8. $f'(\zeta)$ vs Kp

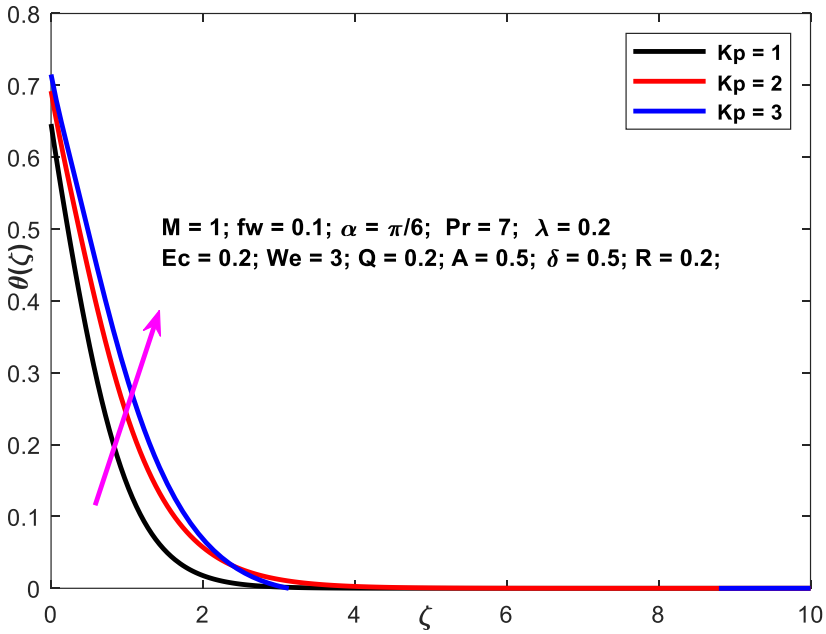

Fig. 9. $\theta(\zeta)$ vs Kp

Figure 10 shows the influence of the Prandtl number (Pr) on a temperature curve. Increases in Pr seem to reduce the fluid's thermal diffusivity, leading to a slower rate at which heat can penetrate into and across the fluid.

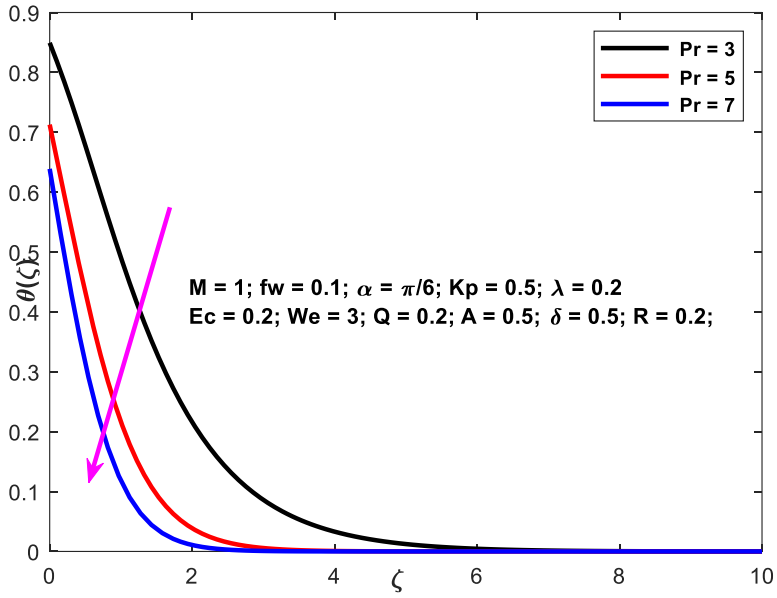

Fig. 10. $\theta(\zeta)$ vs Pr

Figure 11 the impact of Eckert number on the temperature profile. In this figure, we observed that a rise in the viscous dissipation parameter results in an enhancement in the temperature profile. This is because heat energy is stored in the liquid as a result of the frictional heating that takes place.

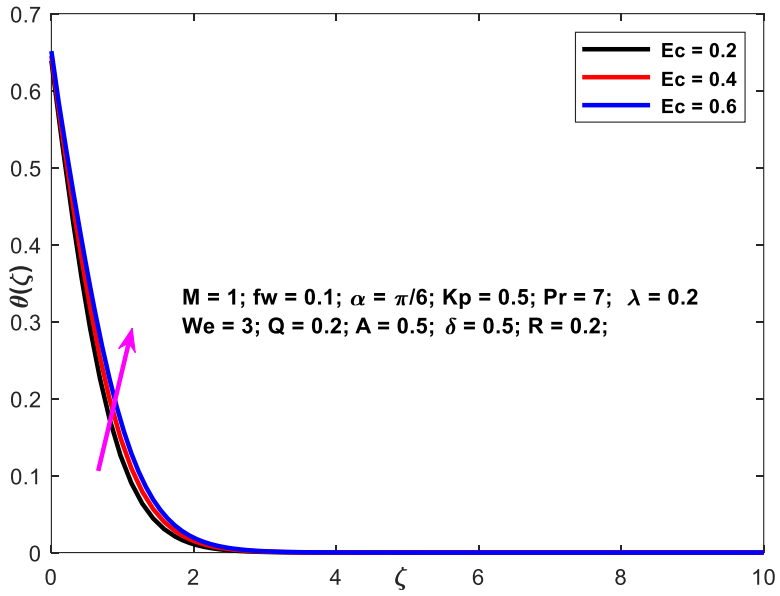

Fig. 11. $\theta(\zeta)$ vs Ec

The effects of the Weinessberg parameter on the temperature profile are shown in Figure 12. Because the W lowers the temperature profile, the thickness of the temperature boundary layer drops, which in turn reduces the amount of heat that is transferred from the surface to the fluid.

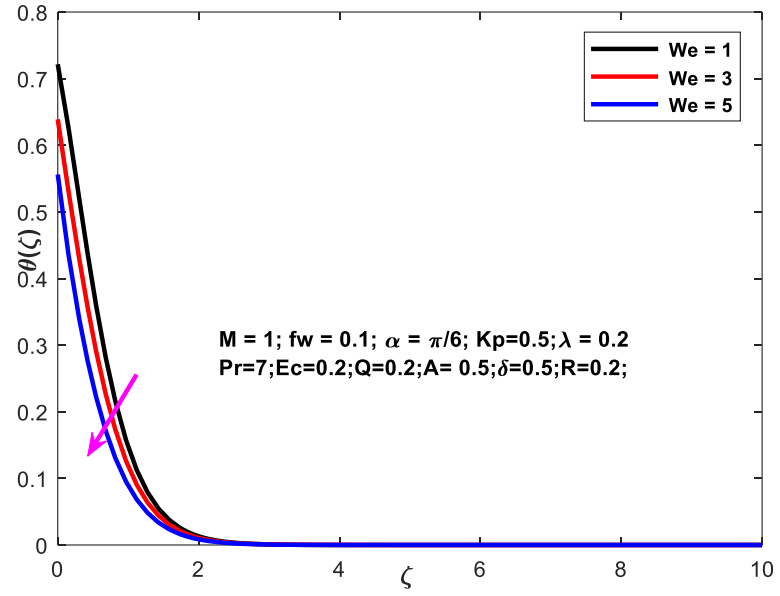

Fig. 12. $\theta(\zeta)$ vs We

Figure 13 and Figure 14 illustrate, respectively, the impacts of the velocity slip parameter on the velocity and temperature curves. With an increase in the velocity slip parameter, which slows down the velocity and raises the temperature as a result, it has been discovered that the temperature rises with an enhancement in the values of A.

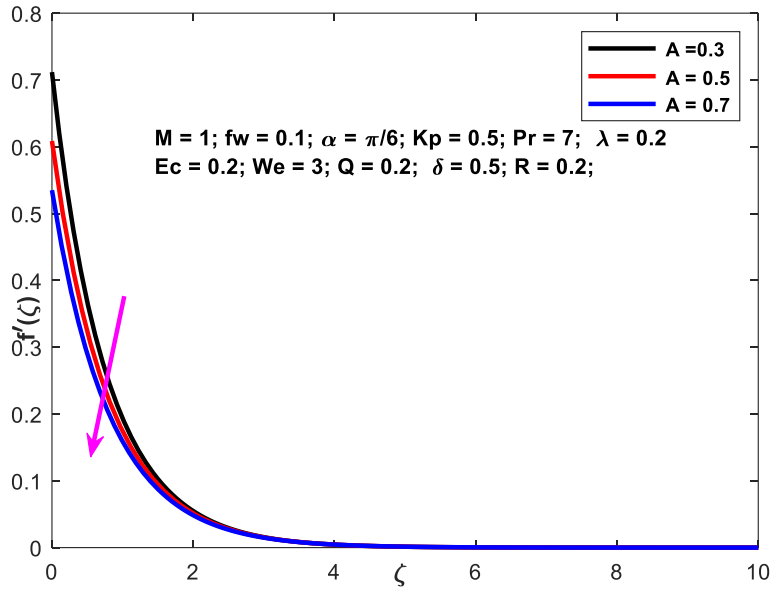

Fig. 13. $f'(\zeta)$ vs A

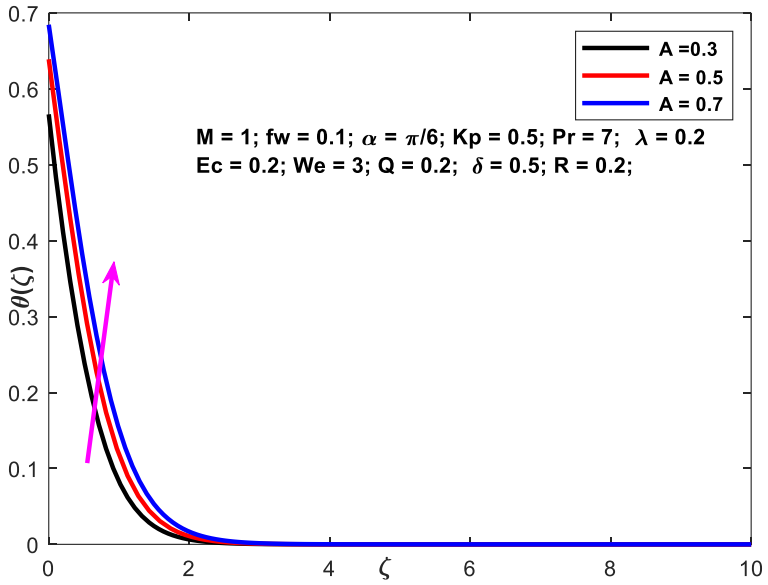

Fig. 14. $\theta(\zeta)$ vs A

The effects of the thermal slip on the temperature are shown in Figure 15. As the value of the thermal slip factor grows, the temperature drops. As a result of the fact that the reason is as δ grows, the temperature either goes up in the free stream or falls at the surface level. Because of this, a drop in thermal boundary layer width also occurs whenever δ values are raised.

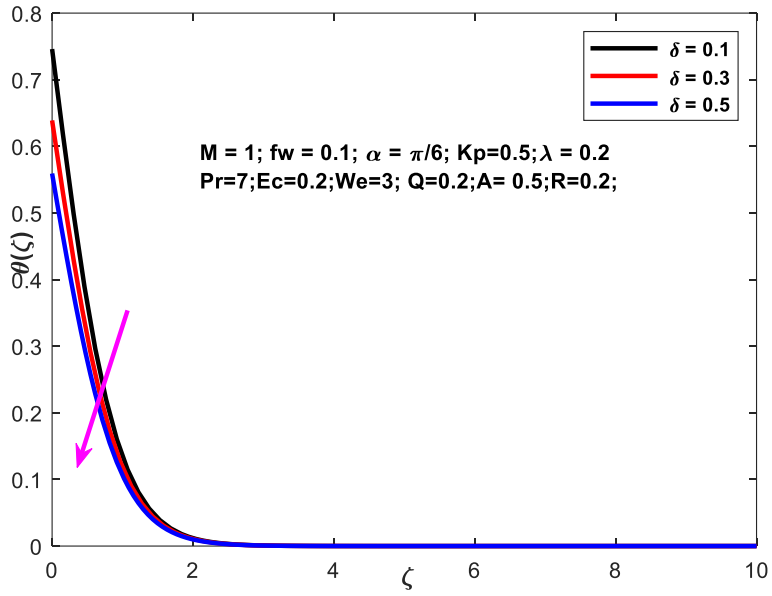

Fig. 15. $\theta(\zeta)$ vs δ

The influence of the radiation factor on the temperature gradients is seen in Figure 16. It has been noticed that when R is increased, there is a corresponding reduction in the temperature profile. This is due to an upsurge in the radiation factor R leads to a reduction in the depth of the thermal boundary layer.

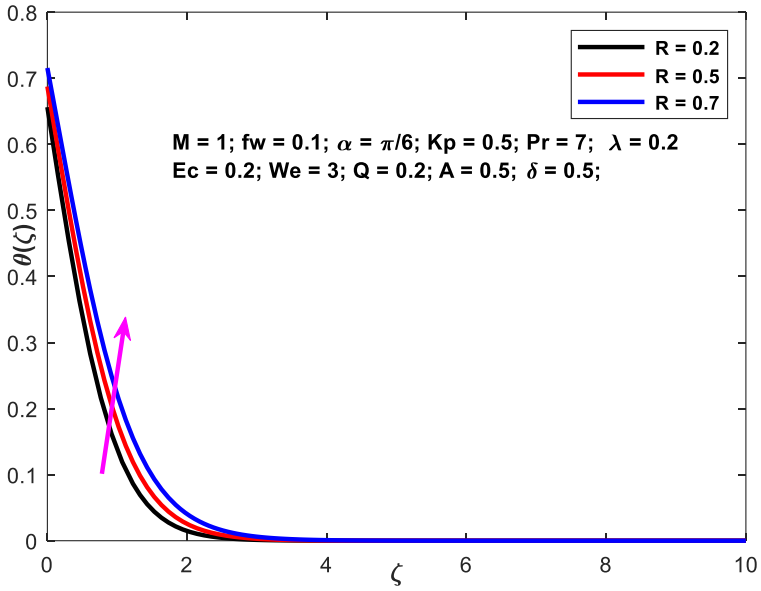

Fig. 16. $\theta(\zeta)$ vs R

Figure 17 displays the physical behavior of the heat source versus the temperature field. Temperature curves show an increase for increasing Q values, as seen by the graph.

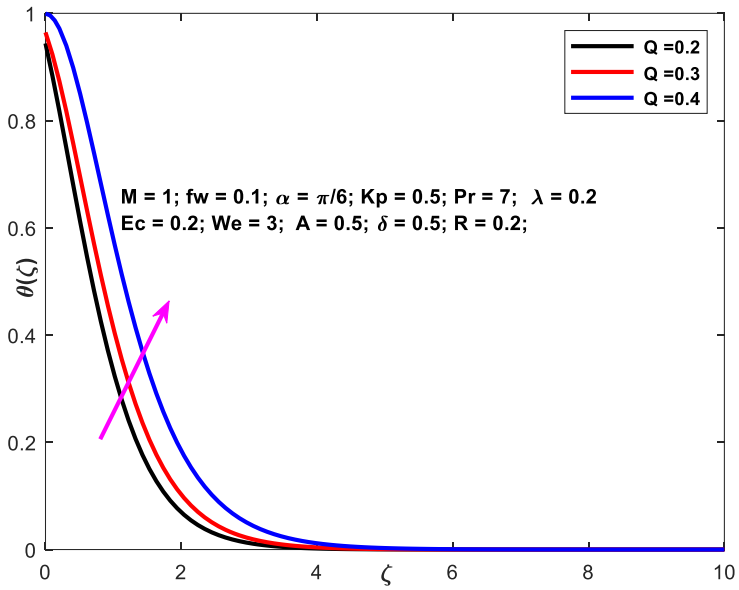

Fig. 17. $\theta(\zeta)$ vs Q

Velocity and Temperature graphs are explored in Figure 18 and Figure 19 for the Williamson factor. The effect of the Williamson factor on the dimensionless velocity and temperature for fixed values of other parameters. These data show that an increase in the non-Newtonian Williamson factor results in a drop in the boundary layer width, which in turn consequences in a decline in the velocity field. In the meanwhile, the temperature is falling.

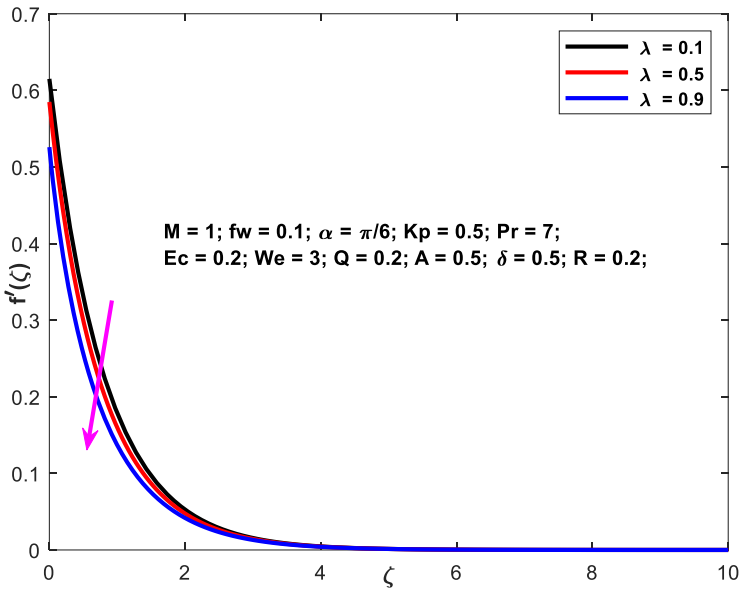

Fig. 18. $f'(\zeta)$ vs λ

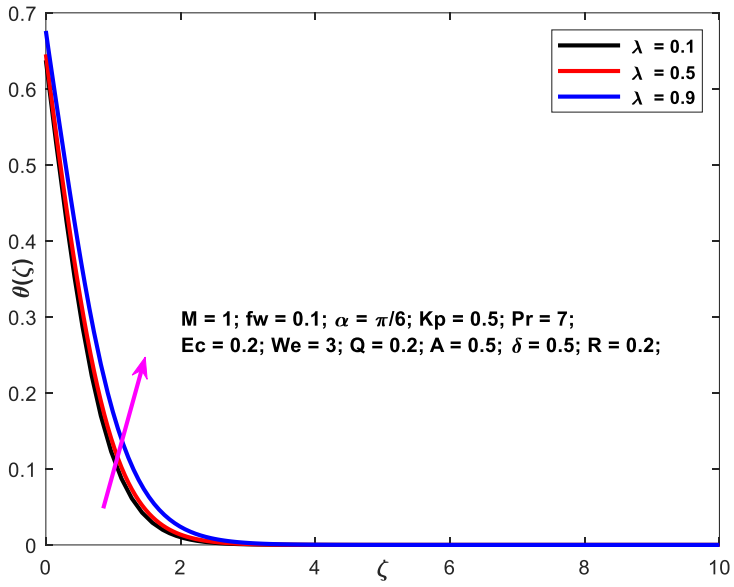

Fig. 19. $\theta(\zeta)$ vs λ

6. Conclusion

In the present study, we investigated the influence of Velocity and Thermal Slips impact on the Williamson fluid flow above a stretching sheet in the existence of inclined magnetic field and Radiation. From the numerical outcomes achieved, some of the interesting outcomes are as follows:

I. The increasing of $M, \alpha, Kp, A, \lambda$ decreases the velocity profile whereas increases the temperature.
II. Increasing fw decreases the velocity profile as well as temperature.
III. With the increasing of Pr, We, δ decreases the temperature
IV. With the increase of radiation parameters R, Q and Ec increases the temperature.

References

[1] Choi, S. Enhancing thermal conductivity of fluids with nanoparticle in Siginer, D. A. &Wanf, H. P. (Eds) Developments and applications of non-Newtonian flows, ASME MD. FED.1995; 231:99-105.
[2] Das, Sarit Kumar, Nandy Putra, Peter Thiesen, and Wilfried Roetzel. "Temperature dependence of thermal conductivity enhancement for nanofluids." *J. Heat Transfer* 125, no. 4 (2003): 567-574. https://doi.org/10.1115/1.1571080
[3] Khan, W. A., and I. Pop. "Boundary-layer flow of a nanofluid past a stretching sheet." *International journal of heat and mass transfer* 53, no. 11-12 (2010): 2477-2483. https://doi.org/10.1016/j.ijheatmasstransfer.2010.01.032
[4] Trisaksri, Visinee, and Somchai Wongwises. "Critical review of heat transfer characteristics of nanofluids." *Renewable and sustainable energy reviews* 11, no. 3 (2007): 512-523. https://doi.org/10.1016/j.rser.2005.01.010
[5] Bachok, Norfifah, Anuar Ishak, and Ioan Pop. "Boundary-layer flow of nanofluids over a moving surface in a flowing fluid." *International Journal of Thermal Sciences* 49, no. 9 (2010): 1663-1668. https://doi.org/10.1016/j.ijthermalsci.2010.01.026
[6] Rana, Puneet, and R. Bhargava. "Flow and heat transfer of a nanofluid over a nonlinearly stretching sheet: a numerical study." *Communications in Nonlinear Science and Numerical Simulation* 17, no. 1 (2012): 212-226. https://doi.org/10.1016/j.cnsns.2011.05.009.
[7] Hassani, M., M. Mohammad Tabar, H. Nemati, G. Domairry, and F. Noori. "An analytical solution for boundary layer flow of a nanofluid past a stretching sheet." *International Journal of Thermal Sciences* 50, no. 11 (2011): 2256-2263. https://doi.org/10.1016/j.ijthermalsci.2011.05.015.

[8] Daniel, Yahaya Shagaiya, Zainal Abdul Aziz, Zuhaila Ismail, and Faisal Salah. "Effects of slip and convective conditions on MHD flow of nanofluid over a porous nonlinear stretching/shrinking sheet." *Australian Journal of Mechanical Engineering* 16, no. 3 (2018): 213-229. https://doi.org/10.1080/14484846.2017.1358844

[9] Das, Kalidas, Pinaki Ranjan Duari, and Prabir Kumar Kundu. "Nanofluid flow over an unsteady stretching surface in presence of thermal radiation." *Alexandria engineering journal* 53, no. 3 (2014): 737-745. https://doi.org/10.1016/j.aej.2014.05.002

[10] Ferdows, M., S. M. Chapal, and A. A. Afify. "Boundary layer flow and heat transfer of a nanofluid over a permeable unsteady stretching sheet with viscous dissipation." *Journal of Engineering Thermophysics* 23, no. 3 (2014): 216-228. https://doi.org/10.1134/S1810232814030059.

[11] Dogonchi, A. S., K. Divsalar, and D. D. Ganji. "Flow and heat transfer of MHD nanofluid between parallel plates in the presence of thermal radiation." *Computer Methods in Applied Mechanics and Engineering* 310 (2016): 58-76. https://doi.org/10.1016/j.cma.2016.07.003.

[12] Prasad, P. Durga, RVMSS Kiran Kumar, and S. V. K. Varma. "Heat and mass transfer analysis for the MHD flow of nanofluid with radiation absorption." *Ain Shams Engineering Journal* 9, no. 4 (2018): 801-813. https://doi.org/10.1016/j.asej.2016.04.016.

[13] Ibrahim, Wubshet, and Dachasa Gamachu. "Nonlinear convection flow of Williamson nanofluid past a radially stretching surface." *AIP Advances* 9, no. 8 (2019). https://doi.org/10.1063/1.5113688.

[14] Nadeem, S., S. T. Hussain, and Changhoon Lee. "Flow of a Williamson fluid over a stretching sheet." *Brazilian journal of chemical engineering* 30 (2013): 619-625. https://doi.org/10.1590/S0104-66322013000300019.

[15] Srinivasulu, Thadakamalla, and B. Shankar Goud. "Effect of inclined magnetic field on flow, heat and mass transfer of Williamson nanofluid over a stretching sheet." *Case Studies in Thermal Engineering* 23 (2021): 100819. https://doi.org/10.1016/j.csite.2020.100819.

[16] Shah, Zahir, Ebenezer Bonyah, Saeed Islam, Waris Khan, and Mohammad Ishaq. "Radiative MHD thin film flow of Williamson fluid over an unsteady permeable stretching sheet." *Heliyon* 4, no. 10 (2018). https://doi.org/10.1016/j.heliyon.2018.e00825.

[17] Malik, M. Y., and T. Salahuddin. "Numerical solution of MHD stagnation point flow of Williamson fluid model over a stretching cylinder." *International Journal of Nonlinear Sciences and Numerical Simulation* 16, no. 3-4 (2015): 161-164. https://doi.org/10.1515/ijnsns-2014-0035.

[18] Hayat, T., Anum Shafiq, and A. Alsaedi. "Hydromagnetic boundary layer flow of Williamson fluid in the presence of thermal radiation and Ohmic dissipation." *Alexandria Engineering Journal* 55, no. 3 (2016): 2229-2240. https://doi.org/10.1016/j.aej.2016.06.004.

[19] Shafiq, Anum, and T. N. Sindhu. "Statistical study of hydromagnetic boundary layer flow of Williamson fluid regarding a radiative surface." *Results in physics* 7 (2017): 3059-3067.https://doi.org/10.1016/j.rinp.2017.07.077

[20] Bilal, M., M. Sagheer, and S. Hussain. "Numerical study of magnetohydrodynamics and thermal radiation on Williamson nanofluid flow over a stretching cylinder with variable thermal conductivity." *Alexandria engineering journal* 57, no. 4 (2018): 3281-3289. https://doi.org/10.1016/j.aej.2017.12.006.

[21] M. Megahed, Ahmed. "Williamson fluid flow due to a nonlinearly stretching sheet with viscous dissipation and thermal radiation." *Journal of the Egyptian Mathematical Society* 27, no. 1 (2019): 12. https://doi.org/10.1186/s42787-019-0016-y

[22] Khan, W. A., and I. Pop. "Boundary-layer flow of a nanofluid past a stretching sheet." *International journal of heat and mass transfer* 53, no. 11-12 (2010): 2477-2483. https://doi.org/10.1016/j.ijheatmasstransfer.2010.01.032

[23] Reddy Gorla, Rama Subba, and Ibrahim Sidawi. "Free convection on a vertical stretching surface with suction and blowing." Applied Scientific Research 52 (1994): 247-257. https://doi.org/10.1007/BF00853952

[24] Wang, C. Y. "Free convection on a vertical stretching surface." *ZAMM-Journal of Applied Mathematics and Mechanics/Zeitschrift für Angewandte Mathematik und Mechanik* 69, no. 11 (1989): 418-420. https://doi.org/10.1002/zamm.19890691115

[25] Rana, S., M. Junaid, R. Mehmood, and M. M. Bhatti. "Transport of chemical species alongside magnetic pseudoplastic nanomaterial through a porous surface." *Modern Physics Letters B* (2023): 2350062. https://doi.org/10.1142/S0217984923500628.

[26] Dadheech, Amit, Amit Parmar, Krishna Agrawal, Qasem Al-Mdallal, and Surbhi Sharma. "Second law analysis for MHD slip flow for Williamson fluid over a vertical plate with Cattaneo-Christov heat flux." *Case Studies in Thermal Engineering* 33 (2022): 101931. https://doi.org/10.1016/j.csite.2022.101931.

[27] Salahuddin, T., Aaqib Javed, Mair Khan, M. Awais, and Harun Bangali. "The impact of Soret and Dufour on permeable flow analysis of Carreau fluid near thermally radiated cylinder." *International Communications in Heat and Mass Transfer* 138 (2022): 106378. https://doi.org/10.1016/j.icheatmasstransfer.2022.106378

[28] Goud, B. Shankar, P. Pramod Kumar, Bala Siddulu Malga, and Y. Dharmendar Reddy. "FEM to study the radiation, Soret, Dufour numbers effect on heat and mass transfer of magneto-Casson fluid over a vertical permeable plate

in the presence of viscous dissipation." *Waves in Random and Complex Media* (2022): 1-22. https://doi.org/10.1080/17455030.2022.2091809

[29] Srisailam, Batcha, Katkoori Sreeram Reddy, Ganji Narender, and Bala Siddhulu Malga. "The Effect of Viscous Dissipation and Chemical Reaction on the Flow of MHD Nanofluid." *Journal of Advanced Research in Fluid Mechanics and Thermal Sciences* 107, no. 2 (2023): 150-170. https://doi.org/10.37934/arfmts.107.2.150170

[30] Jaffrullah, Shaik, Wuriti Sridhar, and G. Raghavendra Ganesh. "MHD Radiative Casson Fluid Flow through Forchheimer Permeable Medium with Joule Heating Influence." *CFD Letters* 15, no. 8 (2023): 179-199. https://doi.org/10.37934/cfdl.15.8.179199.

[31] Kota, Santhi Kumari Dharani, Venkata Subrahmanyam Sajja, and Perugu Mohana Kishore. "Transient MHD Flows Through an Exponentially Accelerated Isothermal Vertical Plate with Viscous Dissipation and Heat Source Embedded in a Porous Medium." *Journal of Advanced Research in Fluid Mechanics and Thermal Sciences* 106, no. 2 (2023): 153-166. https://doi.org/10.37934/arfmts.106.2.153166.

[32] Bejawada, Shankar Goud, Yanala Dharmendar Reddy, Kanti Sandeep Kumar, and Epuri Ranjith Kumar. "Numerical solution of natural convection on a vertical stretching surface with suction and blowing." *Int. J. Heat Tech* 39, no. 5 (2021): 1469-1474. https://doi.org/10.18280/ijht.390508

[33] Iyoko, Michael, and Bakai Ishola Olajuwon. "Study on Impact of Magnetic Dipole and Thermal Radiation on Flow/Heat Transfer of Jeffery Fluid over Stretching Sheet with Suction/Injection." *Journal of Advanced Research in Fluid Mechanics and Thermal Sciences* 104, no. 1 (2023): 65-83. https://doi.org/10.37934/arfmts.104.1.6583

[34] Goud, B. Shankar, Pudhari Srilatha, D. Mahendar, Thadakamalla Srinivasulu, and Yanala Dharmendar Reddy. "Thermal radiation effect on thermostatically stratified MHD fluid flow through an accelerated vertical porous plate with viscous dissipation impact." *Partial Differential Equations in Applied Mathematics* 7 (2023): 100488. https://doi.org/10.1016/j.padiff.2023.100488

[35] Usman, Abubakar, Siti Sabariah Abas, Nurul Aini Jaafar, Muhammad Hassan Muhammand, and Mustafa Mamat. "A Model on Free Convective Casson Fluid Flow Past a Permeable Vertical Plate with Gyrotactic Microorganisms." *Journal of Advanced Research in Fluid Mechanics and Thermal Sciences* 105, no. 2 (2023): 31-50. https://doi.org/10.37934/arfmts.105.2.3150